ISSN 0915-633X

INTERNATIONAL ATOMIC ENERGY AGENCY

SIXTEENTH IAEA FUSION ENERGY CONFERENCE

Montréal, Canada, 7-11 October 1996

IAEA-CN-64/O1-7

NATIONAL INSTITUTE FOR FUSION SCIENCE

Overview of Helical Systems

A. Iiyoshi

(Received - Sep. 27, 1996)

NIFS-453 Sep. 1996

RESEARCH REPORT
NIFS Series

NAGOYA, JAPAN

INTERNATIONAL ATOMIC ENERGY AGENCY

SIXTEENTH IAEA FUSION ENERGY CONFERENCE

Montréal, Canada, 7–11 October 1996

IAEA-CN-64/ O1-7

Overview of Helical Systems

A. Iiyoshi

National Institute for Fusion Science, Nagoya 464-01, Japan

Keywords: Helical System, Global Confinement, Confinement Improvement, High β, Divertor, Heating Development, Future Plan

IAEA-CN-64/O1-7

Overview of Helical Systems

Abstract

Recent experimental results, mainly from heliotron/torsatron devices and an advanced stellarator, are reviewed. An international helical system data base on the energy confinement time has been compiled; the confinement time scaling is similar to the tokamak L-mode. Improved confinement regimes, i.e., high T_i mode, pellet mode, H-mode, and re-heat mode, have also been investigated. In L-mode and improved confinement regimes the energy confinement scaling has a favorable density dependence, and the operating density limit by radiation collapse in helical devices has a much steeper magnetic field dependence than in tokamaks. The maximum attainable β of about 2% is not limited by MHD instabilities but by the absorbed heating power. Investigations of divertor configurations, including local island divertors and natural island divertors, showed that next generation devices will have a good prospect for steady state operations. Based on these results next generation devices (LHD and WVII-X) with a major radius in the range, 4 - 5.5m, have been either under construction or approved for construction. A small Heliac has started its operation, and another has been under construction. A small modular stellarator with a quasi-helical symmetry has also been under construction.

1. Introduction

Experimental investigations have been made in a variety of helical devices. Maximum machine parameters of heliotron/torsatron-type devices and an advanced stellarator [1 ~ 4] fall into the following ranges: the machine major radius, R_0=2-2.2m, plasma minor radius, a_p=0.2-0.3m, magnetic field, B_0=2.5T, and absorbed heating power, P_{abs}=3-4MW. The maximum plasma parameters obtained to date are as follows: the central electron temperature, $T_e(0)$=3keV, central ion temperature, $T_i(0)$=1.6keV, line-averaged density, n_e=2-3$\times 10^{20}$m^{-3}, volume-averaged β, $<\beta>$=2.1%, and energy confinement time, τ_E=40ms (these parameters have not been obtained simultaneously). A main thrust of these experimental investigations has been to exploit to advantage the magnetic configurations characteristic to helical devices in improving transport, raising β, utilizing various heating methods (especially wave heating), and verifying divertor function.

A next generation device, LHD [5, 6], is approaching the final stage of its construction, and another, WVII-X [7], has been approved for construction. Small machines of a fully three dimensional axis type are expected to extend the experimental knowledge to hitherto unexplored regimes.

Helical devices in operation and under construction are summarized in Table I.

2. Transport Studies

2.1 Global confinement

A major progress in the area of transport studies is the establishment of an empirical scaling law for the global confinement time in helical systems. A database of 859 L-mode discharges from ATF, CHS, Heliotron-E (H-E), WVII-AS, and WVII-A has been compiled, and a regression analysis has been performed [8]. The confinement time data is shown in Fig. 1. The proposed scaling law is given by,

$$\tau_E = 0.079\, a_p^{2.21}\, R_0^{0.65}\, P_{abs}^{-0.59}\, n_e^{0.51}\, B_0^{0.83}\, \iota^{0.40}. \qquad (1)$$

In performing the regression, an ansatz was made that the rotational transform evaluated at r =2a/3 is relevant. A few observations may be made regarding the scaling law. The exponents of independent variables, R_0, a_p, P_{abs}, n_e, and B_0 are similar to those of the LHD-scaling [9]. The density exponent here is somewhat smaller. Predicted τ_E is in a range similar to that for the L-mode in tokamaks. This similarity may reflect the fact that the neoclassical ripple transport is not a major loss mechanism in the discharges included in the data base. (The reduction of ripple transport has been attempted, either by using the radial electric field in heliotron/torsatron devices, or by optimizing ripples in an advanced stellarator.) Confinement in WVII-AS in terms of scaling is better than in ATF, H-E or CHS. But an explicit demonstration of relative advantages of each device must await future experiments in higher temperature and less collisional plasmas. The density dependence of energy confinement time is favorable. However, τ_E has been observed to saturate at high densities. This saturation could be removed by using the re-heat mode (see next section).

Operating at high densities is important for helical devices, because it reduces ripple transport. For this reason, the density limit has been studied intensively. Some results are shown in Fig.2. The density limit in present devices is set by a radiation collapse at the plasma edge, and is given by the following scaling law,

$$n_e \propto B_0^{\,a}\, P_{abs}^{\,b}, \qquad (2)$$

where the exponents, (a, b), are reported as (0.5, 0.5) in a high-heating limit in H-E [9] and nearly (1.0, 0.4) in WVII-AS [10]. The density limit is much higher in a helical device than in a tokamak of a similar size. A possible reason for this is that helical devices do not have current disruptions which are a serious problem at the density limit in tokamaks. The size dependence of density limit is now under investigation by comparing WVII-AS and CHS.

The configuration-dependence of τ_E has been studied. An inward shift of magnetic surfaces has been found favorable in heliotron/torsatron devices [11] as well as in stellarators [12]. An improved heating efficiency [11] and a reduction in the ion neoclassical loss [12] are considered as candidates to explain the improved confinement. Increased shear has also been pointed out to be effective in reducing the anomalous transport when the magnetic axis is shifted in heliotron/torsatron devices [13]. The role of magnetic shear has also been tested on an advanced stellarator. The magnetic shear was reduced or enhanced

in WVII-AS using rf-driven currents, but the impact of the change on confinement was found to be small [14]. An explanation for this discrepancy may be that the region of shear modification was small, and that the negative shear simultaneously enhanced the neoclassical loss because of a substantial reduction in iota. Changes in the magnetic structure have been found to reduce the threshold power for L-H transitions in CHS [15].

Further efforts for confinement improvement are necessary in order to arrive at an attractive reactor design based upon a helical system.

2.2 Improved confinement modes

Improved confinement modes have been studied in helical systems; those observed in CHS, H-E, and WVII-AS are summarized in Table II.

High Ti mode

The high ion temperature mode has been observed in neutral beam heated plasmas in H-E (T_i (0) = 1.1 keV) [16, 17] and WVII-AS (T_i (0) = 1.6 keV) [12] at relatively low densities. The energy confinement time in high T_i mode in these devices is 40% larger than that in L-mode in H-E. High T_i mode plasmas are characterized by peakedness in both ion temperature and electron density profiles. Peaked density profiles in high T_i mode are produced by neutral beam fueling with low wall recycling in H-E, and off-axis electron cyclotron heating (ECH) in WVII-AS [18]. From measurements of the profile of radial electric field, its shear is believed to be responsible for the observed reduction in χ_i (= $0.5 m^2/s$) near the plasma center in H-E.

Pellet mode

Injection of a frozen pellet of working gas was found to be effective in achieving a high central ion temperature in helical devices, just as pellet injection was found to be effective in achieving a high density in tokamaks. This was demonstrated in the pellet injection mode in H-E (T_i (0) = 0.7 keV, $n_e(0) = 7.3 \times 10^{19} m^{-3}$) [19]: the ion temperature profile became peaked, and T_i (0) increased after pellet injection.

H- mode

Transition into the H-mode was clearly observed in WVII-AS [20, 21] and CHS [15, 22]: the intensity of H_α light dropped, and the edge density rose rapidly. However, an increase in energy confinement time of up to 30% was less than that usually observed in divertor tokamaks. At L-to-H transitions, a jump in the poloidal rotation velocity in the electron diamagnetic direction (more negative electric field) was observed also in helical systems. The critical poloidal Mach number, $M_{pol} = v_\theta / v_{thermal}(B/B_\theta)$, at L-to-H or H-to-L transitions was 0.5 - 1.

Re-heat mode

An increase in the stored energy was observed together with density peaking when gas puffing was turned off in a high density regime. This was

called re-heating in CHS [23]. The re-heat mode is characterized by a peaked density profile triggered by the decrease in the neutral density at the plasma edge.

Similarities exist in plasma characteristics between improved confinement modes in helical devices and tokamaks. Density and ion temperature profiles in high T_i mode are similar to those observed in the core enhanced confinement modes in tokamaks (supershot [24], PEP-mode [25], VH-mode [26], high-β_p mode [27]). The existence of a critical M_{pol} suggests that a similar mechanism for H-mode takes place both in helical systems and tokamaks (see [28] for review). The plasma behaves very similarly in re-heat mode in helical devices and in IOC mode in tokamaks [29]. Quantitative performance comparisons of improved modes in helical devices and tokamaks must await studies in LHD plasmas with improved particle confinement at larger size and reduced edge neutral densities made possible by a helical divertor.

2.3 Local transport

The measured electron thermal diffusivity, χ_e, is on the order of 1 - 10 m^2/s in helical devices. The radial profile of diffusivity is relatively flat, or it even increases toward the plasma center [30, 31]. This is in contrast to tokamaks in which the diffusivity decreases sharply toward the plasma center. In L-mode the ion thermal diffusivity, χ_i, is similar to χ_e in its magnitude and profile. In improved modes, however, χ_i decreases toward the plasma center, and central values are 0.5 - 1 m^2/s. These values are close to those observed in improved modes in tokamaks [24]. In general, measured thermal diffusivities are much larger than neoclassical values except near the plasma center at low collisionality, where neoclassical values are large. Theoretical efforts have been made to model the anomalous transport. A nonlinear theory has been developed for a current-diffusive ballooning/interchange mode [32], which gives a qualitative explanation for the transport anomaly.

2.4 Radial electric field

The radial electric field and associated space potential profile have been investigated intensively as a possible means of reducing the ripple loss and preventing confinement degradation in helical systems [33, 34]. These investigations were motivated by the expectation that the ripple loss and other neoclassical transport losses become more important in higher-temperature lower-collisionality plasmas in future devices. The radial electric field depends on both heating scheme and plasma density. Recently a 200kV HIBP measurement started to obtain a radial profile of electric potentials in CHS [35]. A positive field was observed in ECH plasmas, while a negative field was seen in NBI plasmas [33, 35, 36], as shown in Fig.3. In NBI plasmas, the field became more negative as the electron density increased, but the field became less negative as the density decreased. A bifurcation of radial electric field was seen in transitions from the ion root to electron root [37], or in L-to-H transitions [38]. Measurements in low-density plasmas in CHS heated by high-power

ECH suggested the appearance of a potential structure that acts as an internal transport barrier [36]. Some aspects of radial electric field behave in accordance with neoclassical theories. But the magnitude and radial profile of the field do not always agree with predictions of neoclassical theories [28,39].

3. High β Plasma

Design values of the volume-averaged β limit are typically 5 % for next generation helical systems [5 ~ 7]. In present experiments, β values up to 2 % have been achieved with neutral beam injection [40 ~ 43]. This observed experimental limit is close to the theoretical stability limit in H-E, but is far below the theoretical limit in other devices. In CHS experiments, the global energy confinement was not degraded further than that given by eq. (1); the density was increased along with the input power, and the measured magnetic fluctuations did not increase as β increased. Maximum β values in the present CHS experiments are determined by a density limit set by radiation loss and degradation of beam heating efficiency in low magnetic field operations [44].

Development of three-dimensional MHD codes, thanks to recent advances in super-computer technology, enabled greatly improved comparisons of experimental and theoretical equilibria of high β plasmas. A measured dependence of Shafranov shift on the plasma pressure was clearly describable by model MHD calculations [3, 45]. Shafranov shift was observed to be reduced in WVII-AS as expected from the reduction in Pfirsch-Schluter current. This experimental confirmation of a theoretical expectation was one of the most important objectives of configuration optimization in WVII-AS.

Various saturated MHD modes have been studied in helical devices. A burst-type mode in NBI plasmas in CHS was examined with local potential measurements using HIBP [35]. The dynamic structure of pressure driven instabilities was studied in H-E using a 2D tomographic analysis of soft x-ray signals [46]. A similar technique was used for the analysis of a type of Alfven eigenmode (GAE) in NBI plasmas in WVII-AS [47]; no significant fast ion loss was observed to date.

A ballooning instability was recently investigated theoretically for plasmas in helical devices. The instability had been considered less serious in the past because of a favorable magnetic shear structure of helical systems [48].

4. Divertor Study

In a heliotron/torsatron type configuration a built-in separatrix configuration at the free space between helical coils leads to a helical divertor structure. Careful considerations were given in designing LHD to realize a helical divertor also in a relatively low aspect ratio device. Basic function of helical divertors was studied in H-E which has a clearly defined divertor structure due to its high aspect ratio. Profiles of particle and heat fluxes were measured at the plasma boundary, which demonstrated the existence of localized structures at the divertor traces [49].

The boundary field of a modular stellarator does not possess a simple divertor because of overlapping of various mode structures. The island divertor

concept has been developed instead to realize effective divertor function at the boundary. The island divertor was studied in WVII-AS [50] by taking advantage of natural islands in the vicinity of the outermost magnetic surface. Figure 4 shows density profiles within an island near the surface, which demonstrate the presence of a high density plasma within the island when the main plasma density is high enough. This spontaneous increase in the density within the island provides a basis to establish a cold dense plasma in island divertors. Three-dimensional modeling of divertor plasmas is also in progress [51]. The island divertor is considered to be a main candidate for modular systems such as WVII-X.

A similar island divertor, called LID (local island divertor) [52], can be constructed in LHD by introducing a perturbation field to create artificial islands at the plasma boundary. The island structure is designed to enhance the efficiency of a standard pumped divertor. LID is designed to be an alternative to a standard helical divertor for LHD. Preliminary experiments to demonstrate the LID concept were performed in CHS [53]. The main plasma density was observed to decrease, and the plasma flow into, and the gas pressure within, the pumped divertor both increased, when an artificial island structure was created.

5. Development in Heating

ECH is a main heating resource in almost all helical devices. For example, an ECH power density of a few MW/m^3 is expected in L-2M [54]. Long pulse (4667sec) operation of ECH plasma was achieved in ATF by using a 28GHz gyrotron with the injected power of 70kW [55]. The required gyrotron frequency continues to rise as the confining field in present and future devices increases. Recently over-dense plasmas without the electron cyclotron resonance could be heated with ECH in WVII-AS [56]. Here, an O-X-B mode conversion took place under the following parameters: B_0=2.0T, 140GHz, $n_e=1.6\times10^{20}m^{-3}$, while the 2nd harmonic mode cut-off of 140GHz occurs at B_0=2.5T and $n_e=1.2\times10^{20}m^{-3}$.

ICRF alone could sustain plasmas for a maximum RF pulse length of 70ms in CHS. In these experiments electrons were primarily heated via a mode conversion of ion cyclotron wave to ion Bernstein wave in D (H minority of 30%) plasmas [57]. ICRF alone could also sustain deuterium plasmas (H minority of 10%) in WVII-AS and ion tail distribution was observed [58].

6. Future Plan

LHD is in the final stage of its construction; super-conducting helical windings have been completed [59 ~ 61]. The first plasma is scheduled in April 1998 with 1MW ECH and diagnostics for basic plasma parameters. WVII-X, which is fully optimized for a Helias-type reactor, is scheduled to be operational in 2004. The large plasma volume and heating power, and super-conducting magnets in these facilities will open a new era in studies of the plasma confinement and steady-state operations of helical devices. Reactor-relevant plasmas will be realized in these devices. U-2M torsatron with a low helical ripple is waiting for resumption of operation [62]. A small Heliac has started its

operation (H-1[63]), and another is in the final stage of construction (TJ-II [64]). In these Heliac devices, plasma confinement in configurations with a fully three dimensional magnetic axis will be studied; the l=1 component is a key element for stellarator optimization. A small modular stellarator, HSX [65], based on the principle of quasi-helical symmetry [66] is under construction in USA. This principle results in the absolute confinement of particle orbits.

7. Summary

Helical systems have a variety of magnetic configurations. Although the systems have well-known inherent advantages, i.e., no major disruptions and steady state operations, there remain key issues to be addressed: improving confinement by a significant factor, achieving high β (>5%), and demonstrating steady state operations with appropriate exhaust. These issues are expected to be solved in the next generation devices, LHD and WVII-X, which are optimized on the basis of results from presently operating heliotron/torsatron devices and an advanced stellarator, respectively. A new trend based on stellarator optimization is also emerging. Vigorous investigations of helical systems are currently in progress from both physics and engineering standpoints.

Acknowledgements

The author would like to thank members of the fusion research community working on helical systems, who have kindly provided valuable information for this review, and Prof. F. Wagner for valuable comments.

References

[1] UO, K., et al., in Plasma Physics and Controlled Nuclear Fusion Research (Proc. 9th Int. Conf., 1982, Baltimore), Vol.II, p.209.
[2] MATSUOKA, K., et al., in Plasma Physics and Controlled Nuclear Fusion Research (Proc. 12th Int. Conf., 1988, Nice), Vol.II, p.411.
[3] RENNER, H., et al., in Plasma Physics and Controlled Nuclear Fusion Research (Proc. 13th Int. Conf., 1990, Washington), Vol.II, p.439.
[4] FUJIWARA, M., in Plasma Physics and Controlled Nuclear Fusion Research (Proc. 14th Int. Conf., 1992, Wurzburg), Vol.IV, p.23.
[5] IIYOSHI, A., et al., Fusion Technology 17 (1990) 169.,
[6] MOTOJIMA, O., et al., in Plasma Physics and Controlled Nuclear Fusion Research (Proc. 13th Int. Conf., 1990, Washington), Vol.III, p.513.
[7] GRIEGER, G., et al., in Plasma Physics and Controlled Nuclear Fusion Research (Proc. 12th Int. Conf., 1988, Nice), Vol.II, p.369.
[8] STROTH, U., et al., Nucl. Fusion 36 (1996) 1063.
[9] SUDO, S., et al., Nucl. Fusion 30 (1990) 11.
[10] HOFMANN, J., et al., invited paper for 23rd EPS Conference (Kiev, 1996), to be published in Plasma Phys. Contr. Fusion.
[11] KANEKO, O., et al., in Plasma Physics and Controlled Nuclear Fusion Research (Proc. 13th Int. Conf., 1990, Washington), Vol.II, p.473.

[12] WELLER, A. et al., to be published in Fusion Engineering and Design (Proc. 7th Int. Toki Conf. on Plasma Physics and Controlled Nuclear Fusion, Toki, 1995).
[13] ITOH, K., et al., in Plasma Physics and Controlled Nuclear Fusion Research (Proc. 15th Int. Conf., 1994, Seville) Vol.III, p.391.
[14] ERCKMANN, V., et al., in Proc. 22nd Euro. Conf. on Controlled Fusion and Plasma Physics, Bournemouth, 1995, Vol.19C, Part I, p.389.
[15] TOI, K., et al., in Plasma Physics and Controlled Nuclear Fusion Research (Proc. 14th Int. Conf., 1992, Wurzburg), Vol.II, p.461.
[16] IDA, K., et al., Phys. Rev. Lett. 76 (1996) 1268 .
[17] OBIKI, T., et al., in Plasma Physics and Controlled Nuclear Fusion Research (Proc. 15th Int. Conf., 1994, Seville), Vol.I, p.757.
[18] KUEHNER, G. et al., in Plasma Physics and Controlled Nuclear Fusion Research (Proc. 15th Int. Conf., 1994, Seville), Vol.I, p.145.
[19] IDA, K.et al., IAEA-CN-64/CP-5, these Proceedings.
[20] ERCKMANN, V., et al., Phys. Rev. Lett. 70 (1993) 2086.
[21] WAGNER, F., et al., Plasma Phys. Contr. Fusion 36 (1994) A61
[22] TOI, K., et al., Plasma Phys. Contr. Fusion 36 (1994) A117
[23] MORITA, S., et al., in Plasma Physics and Controlled Nuclear Fusion Research (Proc. 14th Int. Conf., 1992, Wurzburg), Vol.II, p.515.
[24] HAWRYLUK, R.J., et al., Plasma Phys. Contr. Fusion 33 (1991) 1509.
[25] KEILHACKER, M., et al., Plasma Phys. Contr. Fusion 33 (1991) 1453.
[26] OSBORNE, T.H., et al., Plasma Phys. Contr. Fusion 36 (1994) A237.
[27] KOIDE, Y.et al., in Plasma Physics and Controlled Nuclear Fusion Research (Proc. 15th Int. Conf., 1994, Seville), Vol.I, p.199.
[28] For the review of the electric field and improved confinement, see; ITOH, K., et al., Plasma Phys. Contr. Fusion 38 (1996) 1., ITOH, S-I., et al., J. Nucl. Mat. 220-222 (1995) 117.
[29] SOLDNER, F.X., et al., Phys. Rev. Lett. 61 (1988) 1105.
[30] RINGLER, H., et al., Plasma Phys. Control. Fusion 32 (1990) 933.
[31] IGUCHI, H., et al., in Proc. 17th Euro. Conf. on Controlled Fusion and Plasma Physics, Amsterdam, 1990, Vol.14B, Part II, p.451.
[32] ITOH, K., et al., Phys. Rev. Lett. 69 (1992) 1050 ITOH, K., et al., Plasma Phys. Contr. Fusion 36 (1994) 1501.
[33] KONDO, K., et al., Rev. Sci. Instrum, 59, (1988) 1533.
[34] WOBIG, H., et al., in Plasma Physics and Controlled Nuclear Fusion Research (Proc. of 11th Int. Conf., Kyoto, 1986) Vol.II p.369.
[35] FUJISAWA, A., et al., IAEA-CN-64/C1-5(C), these Proceedings.
[36] IDA, K., et al., Phys. Fluids B3 (1991) 515 and Phys. Fluids B4 (1992) 1360.
[37] IDEI, H., et al., Phys. Rev. Lett. 71 (1993) 2220.
[38] HOFMANN, J.V., et al., in Proc. 21st Euro. Conf. on Controlled Fusion and Plasma Physics, Montpellier, 1994, Vol.18B, Part I, p.392.
[39] SANUKI, H., et al., Physica Scripta 52 (1995) 461.

[40] MOTOJIMA, O., et al., Nucl. Fusion 25 (1985) 1783.
[41] MURAKAMI, M., et al., Phys. Fluids B3 (1991) 2261.
[42] OKAMURA, S., et al., Nucl. Fusion 35 (1995) 283.
[43] KICK, M., et al., IAEA-CN-64/C1-4, these Proceedings.
[44] MURAKAMI, S., et al., IAEA-CN-64/CP-6, these Proceedings.
[45] YAMADA, H., et al., Nucl. Fusion 32 (1992) 25.
[46] ZUSHI, H., et al., IAEA-CN-64/CP-4, these Proceedings.
[47] WELLER, A., et al., Phys. Rev. Lett. 72 (1994) 1220.
[48] NAKAJIMA, N., et al., IAEA-CN-64/D3-6, these Proceedings.
[49] MATSUURA, H., Nucl.Fusion 32 (1992) 405.
[50] GRIGULL, P., et al., IAEA-CN-64/C1-1(R), these Proceedings., GRIGULL, P., et al., presented at PSI Conference (St. Raphael, 1996); to be published in J. Nucl. Mat.
[51] FENG, Y., et al., presented at PSI Conference (St. Raphael, 1996); to be published in J. Nucl. Mat.
[52] KOMORI, A., et al., in Plasma Physics and Controlled Nuclear Fusion Research (Proc. 15th Int. Conf., 1994, Seville), Vol.II, p.773.
[53] KOMORI, A., et al., IAEA-CN-64/C1-2, these Proceedings.
[54] GREBENSHCHIKOV, S.E., et al., IAEA-CN-64/CP-10, these Proceedings.
[55] BIGELOW, T.S., et al., Bull. Am. Phys.Soc. 39 (1994) 1603.
[56] ERCKMANN, V., et al., IAEA-CN-64/CP-1, these Proceedings.
[57] NISHIMURA, K., et al., in Plasma Physics and Controlled Nuclear Fusion Research (Proc. 15th Int. Conf., 1994, Seville), Vol.I, p.783.
[58] HARTMANN, D., et al., Stellarator News, Issue 44 (1996) 5.
[59] IIYOSHI, A., et al., Phys. of Plasmas, 2 (1995) 2349.
[60] FUJIWARA, M., et al., Transactions of Fusion Technology 27 (1995) 58.
[61] MOTOJIMA, O., et al., IAEA-CN-64/G2-4, these Proceedings.
[62] PAVLICHENKO, O.S., et al., Plasma Phys. Control. Fusion 35 (1993) B223.
[63] BLACKWELL, B.D., et al., in Plasma Physics and Controlled Nuclear Fusion Research (Proc. 15th Int. Conf., 1994, Seville), Vol.II, p.337.
[64] ASCASIBAR, E., et al., in Plasma Physics and Controlled Nuclear Fusion Research (Proc. 15th Int. Conf., 1994, Seville), Vol.I, p.749.
[65] MATTHEWS, P.G., et al., in Proc. 10th Stellarator Wokshop (1995) p.167.
[66] NUEHRENBERG, J., et al., Phys. Lett. A 129 (1988) 113.

Figure Captions

Fig.1. Global energy confinement time scaling based on the international helical system data base. SI units are used; τ_E(s), a_p(m), R_0(m), P_{abs}(MW), $n_e(10^{19}$m-3), B_0(T). (Based on [8])

Fig.2. (a) Density limit as a function of magnetic field strength. (b) Density limit

as a function of NBI power. In comparing to the Greenwald limit, the plasma current is replaced by the rotational transform in W7-AS. (Based on [10])

Fig.3. (a) Potential and (b) Electric field profiles of ECH and NBI plasmas for R_{ax} = 0.921m and B_0 = 0.9T in CHS. The electric field profile of a medium density plasma shows a strong shear (solid line). The expected electric field from a neoclassical theory is shown by the dashed-dotted line. (Quoted from [35])

Fig.4. Electron density profiles inside natural islands for various electron densities of the main plasma in WVII-AS. When the main plasma density is high the density inside the island becomes peaked. (Quoted from [50])

Table I. Machine parameters of helical devices in operation and under construction.

	R_0 (m)	a_p (m)	V_p (m^3)	B_0 (T)	P_{heat} (MW)	remarks on configuration
H-E (Kyoto)	2.2	0.2	1.74	2.0	7	l=2, m=19, high ι, high shear
CHS (Nagoya)	1.0	0.2	0.79	2.0	3	l=2, m=8, medium ι, magnetic well
L2-M (Moscow)	1.0	0.11	0.24	1.5	0.9	l=2, m=14, medium ι, medium shear
U-3M (Kharkov)	1.0	0.13	0.33	2.0	0.2	l=3, m=9, open helical divertor
CAT (Auburn)	0.53	0.1	0.10	0.1		l=1+2, m=5
U-2M (Kharkov)	1.7	0.22	1.62	2.4	2.0	l=2, m=4, low helical ripple
LHD (Toki)	3.9	0.6	28	3.0	28	l=2, m=10, SC, closed helical divertor
WVII-AS (Garching)	2.0	0.2	1.58	2.5	5	m=5, low shear, low P-S current
WVII-X (Greifswald)	5.5	0.5	27	2.5		m=5, SC, optimization
HSX (Madison)	1.2	0.15	0.53	1.25	0.2	m=4, quasi-helical symmetry
H-1 (Canberra)	1.0	0.2	0.79	1.0	0.2	m=3 heliac
TJ-IU (Madrid)	0.6	0.1	0.12	0.7	0.6	l=1, m=6
TU-Heliac (Sendai)	0.48	0.07	0.05	0.35		m=4 heliac
TJ-II (Madrid)	1.5	0.2	1.18	1.0		m=4 flexible heliac

(l = multipolarity, m = toroidal period number)

TABLE II. Improved confinement modes observed in CHS, H-E and WVII-AS

operating electron density	mode	CHS	H-E	WVII-AS
low density	high T_i mode		$T_i^{CXS}(0) = 0.85$ keV $\Delta\tau_E \leq 40\%$ $\Delta T_i(0) \leq 80\%$ $\chi_i(0.1) = 0.5 m^2/s$ $n_e = 2.5 \times 10^{19} m^{-3}$ [16] $T_i^{NPA}(0) = 1.1$ keV [17]	$T_i^{NPA,CXS}(0)$ $= 1.6$ keV [12]
medium density	pellet mode		$T_i^{CXS}(0) = 0.7$ keV $\Delta T_i(0) \leq 60\%$ $\chi_i(0.1) = 0.7 m^2/s$ $n_e = 4 \times 10^{19} m^{-3}$ [19]	
	H-mode	$\Delta\tau_E = 15\%$ $n_e = 3 \times 10^{19} m^{-3}$ [15,22]		$\Delta\tau_E \leq 30\%$ $M_{pol} = 0.5 - 1$ $n_e = 5 \times 10^{19} m^{-3}$ [20,21]
high density	reheat	$\Delta\tau_E \leq 20\%$ $n_e = 6 \times 10^{19} m^{-3}$ [23]		

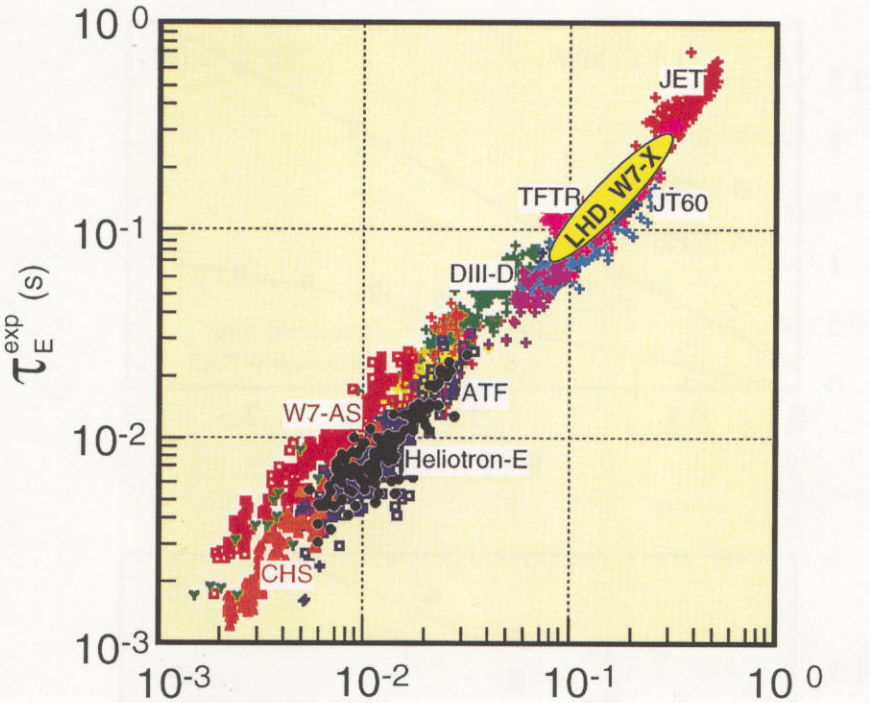

IAEA-CN-64/O1-7 Iiyoshi Fig.1

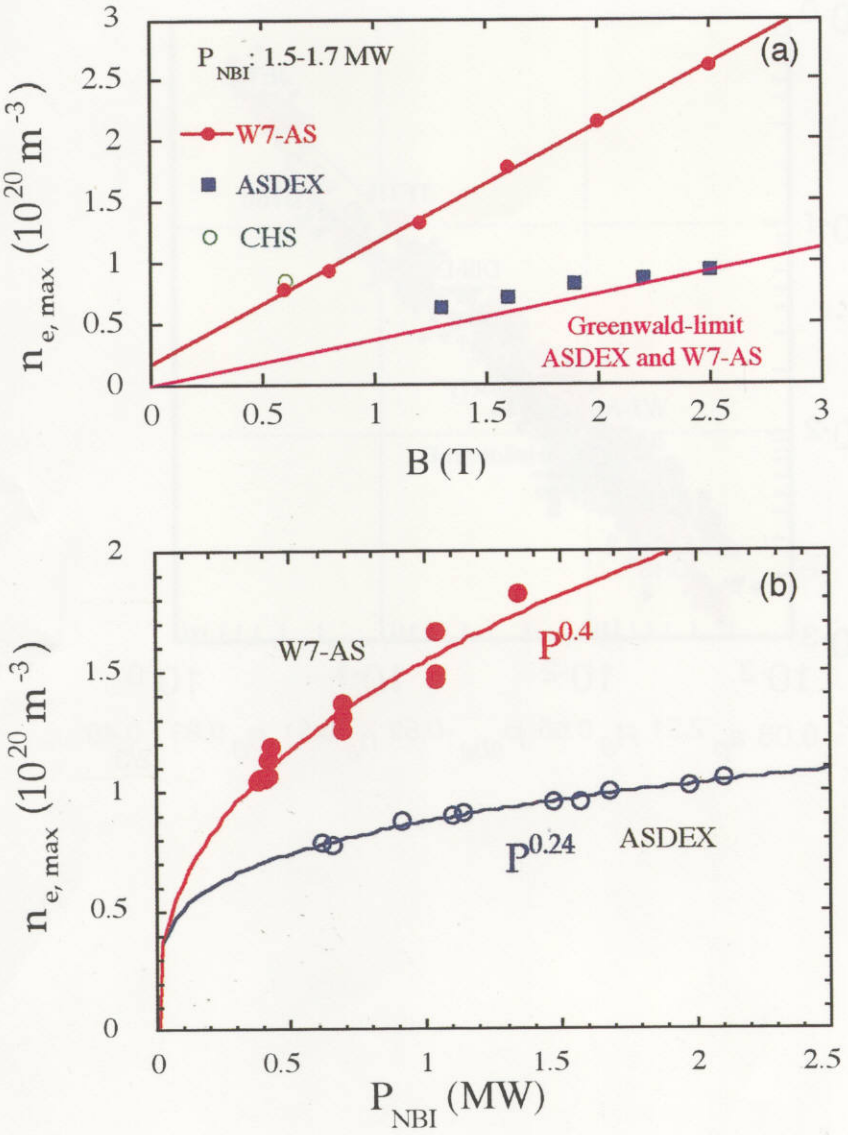

IAEA-CN-64/O1-7 Iiyoshi Fig.2

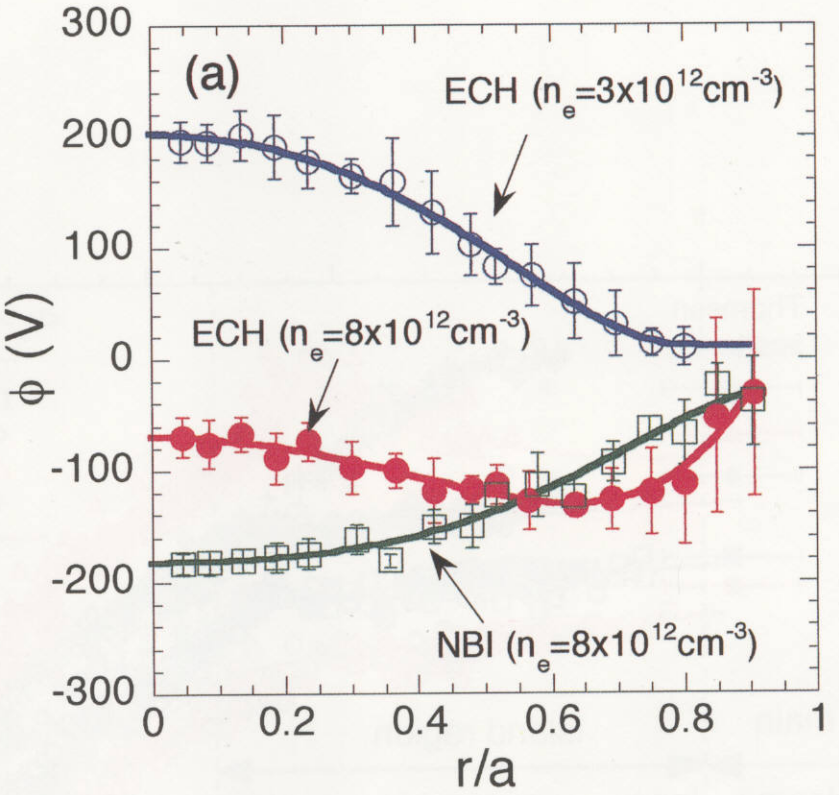

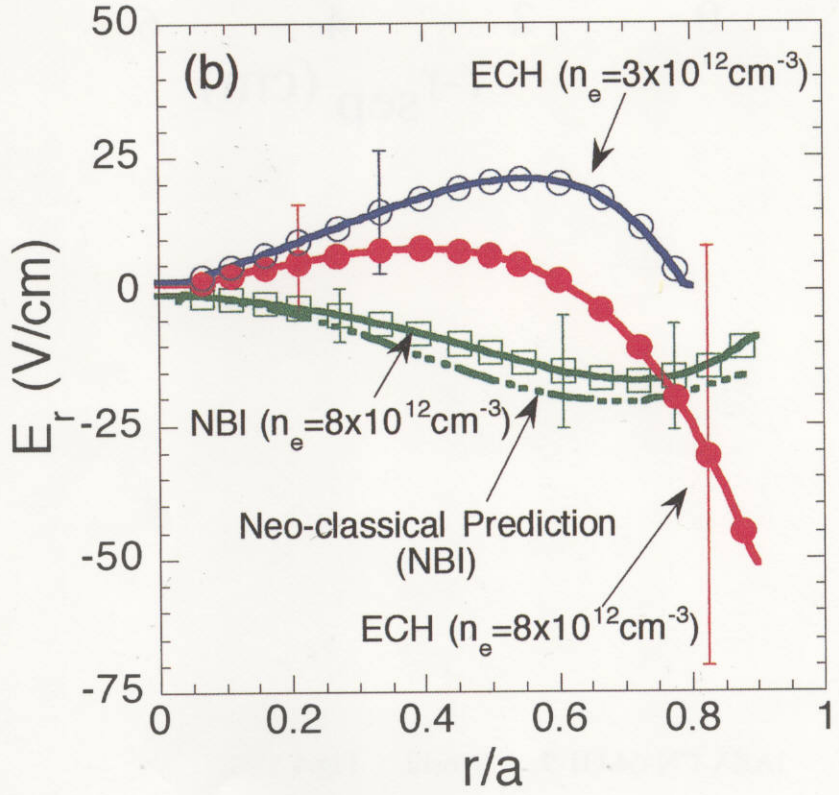

IAEA-CN-64/O1-7 Iiyoshi Fig.3

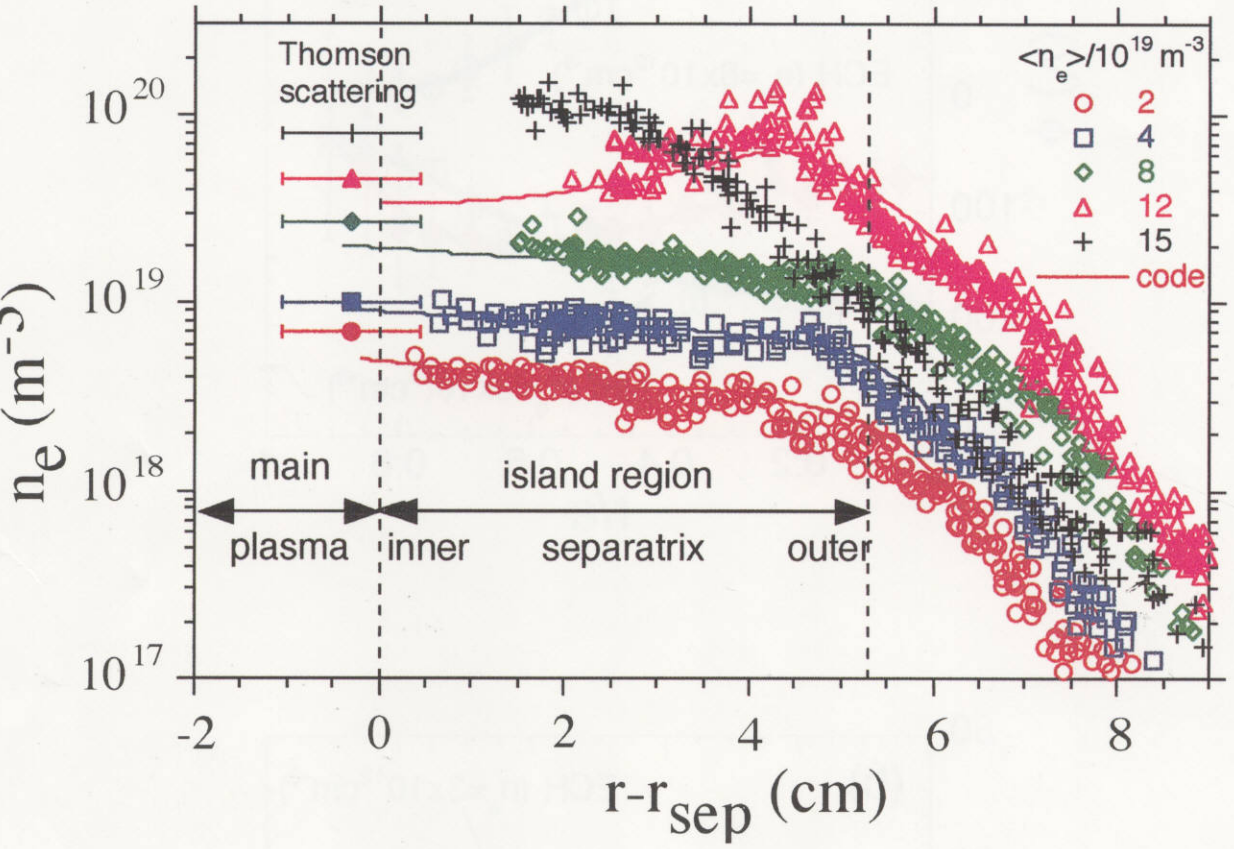

IAEA-CN-64/O1-7 Iiyoshi Fig.4

Recent Issues of NIFS Series

NIFS-416 M. Iwase, K. Ohkubo, S. Kubo and H. Idei
Band Rejection Filter for Measurement of Electron Cyclotron Emission during Electron Cyclotron Heating; May 1996

NIFS-417 T. Yabe, H. Daido,T. Aoki, E. Matsunaga and K. Arisawa,
Anomalous Crater Formation in Pulsed-Laser-Illuminated Aluminum Slab and Debris Distribution; May 1996

NIFS-418 J. Uramoto,
Extraction of K^- Mesonlike Particles from a D_2 Gas Discharge Plasma in Magnetic Field; May 1996

NIFS-419 J. Xu, K. Toi, H. Kuramoto, A. Nishizawa, J. Fujita, A. Ejiri, K. Narihara, T. Seki, H. Sakakita, K. Kawahata, K. Ida, K. Adachi, R. Akiyama, Y. Hamada, S. Hirokura, Y. Kawasumi, M. Kojima, I. Nomura, S. Ohdachi, K.N. Sato
Measurement of Internal Magnetic Field with Motional Stark Polarimetry in Current Ramp-Up Experiments of JIPP T-IIU; June 1996

NIFS-420 Y.N. Nejoh,
Arbitrary Amplitude Ion-acoustic Waves in a Relativistic Electron-beam Plasma System; July 1996

NIFS-421 K. Kondo, K. Ida, C. Christou, V.Yu.Sergeev, K.V.Khlopenkov, S.Sudo, F. Sano, H. Zushi, T. Mizuuchi, S. Besshou, H. Okada, K. Nagasaki, K. Sakamoto, Y. Kurimoto, H. Funaba, T. Hamada, T. Kinoshita, S. Kado, Y. Kanda, T. Okamoto, M. Wakatani and T. Obiki,
Behavior of Pellet Injected Li Ions into Heliotron E Plasmas; July 1996

NIFS-422 Y. Kondoh, M. Yamaguchi and K. Yokozuka,
Simulations of Toroidal Current Drive without External Magnetic Helicity Injection; July 1996

NIFS-423 Joong-San Koog,
Development of an Imaging VUV Monochromator in Normal Incidence Region; July 1996

NIFS-424 K. Orito,
A New Technique Based on the Transformation of Variables for Nonlinear Drift and Rossby Vortices; July 1996

NIFS-425 A. Fujisawa, H. Iguchi, S. Lee, T.P. Crowley, Y. Hamada, H. Sanuki, K. Itoh, S. Kubo, H. Idei, T. Minami, K. Tanaka, K. Ida, S. Nishimura, S. Hidekuma, M. Kojima, C. Takahashi, S. Okamura and K. Matsuoka,
Direct Observation of Potential Profiles with a 200keV Heavy Ion Beam Probe and Evaluation of Loss Cone Structure in Toroidal Helical Plasmas on

the Compact Helical System; July 1996

NIFS-426 H. Kitauchi, K. Araki and S. Kida,
Flow Structure of Thermal Convection in a Rotating Spherical Shell; July 1996

NIFS-427 S. Kida and S. Goto,
Lagrangian Direct-interaction Approximation for Homogeneous Isotropic Turbulence; July 1996

NIFS-428 V.Yu. Sergeev, K.V. Khlopenkov, B.V. Kuteev, S. Sudo, K. Kondo, F. Sano, H. Zushi, H. Okada, S. Besshou, T. Mizuuchi, K. Nagasaki, Y. Kurimoto and T. Obiki,
Recent Experiments on Li Pellet Injection into Heliotron E; Aug. 1996

NIFS-429 N. Noda, V. Philipps and R. Neu,
A Review of Recent Experiments on W and High Z Materials as Plasma-Facing Components in Magnetic Fusion Devices; Aug. 1996

NIFS-430 R.L. Tobler, A. Nishimura and J. Yamamoto,
Design-Relevant Mechanical Properties of 316-Type Stainless Steels for Superconducting Magnets; Aug. 1996

NIFS-431 K. Tsuzuki, M. Natsir, N. Inoue, A. Sagara, N. Noda, O. Motojima, T. Mochizuki, T. Hino and T. Yamashina,
Hydrogen Absorption Behavior into Boron Films by Glow Discharges in Hydrogen and Helium; Aug. 1996

NIFS-432 T.-H. Watanabe, T. Sato and T. Hayashi,
Magnetohydrodynamic Simulation on Co- and Counter-helicity Merging of Spheromaks and Driven Magnetic Reconnection; Aug. 1996

NIFS-433 R. Horiuchi and T. Sato,
Particle Simulation Study of Collisionless Driven Reconnection in a Sheared Magnetic Field; Aug. 1996

NIFS-434 Y. Suzuki, K. Kusano and K. Nishikawa,
Three-Dimensional Simulation Study of the Magnetohydrodynamic Relaxation Process in the Solar Corona. II.; Aug. 1996

NIFS-435 H. Sugama and W. Horton,
Transport Processes and Entropy Production in Toroidally Rotating Plasmas with Electrostatic Turbulence; Aug. 1996

NIFS-436 T. Kato, E. Rachlew-Källne, P. Hörling and K.-D Zastrow,
Observations and Modelling of Line Intensity Ratios of OV Multiplet Lines for 2s3s 3S1 - 2s3p 3Pj; Aug. 1996

NIFS-437 T. Morisaki, A. Komori, R. Akiyama, H. Idei, H. Iguchi, N. Inoue, Y. Kawai, S.

Kubo, S. Masuzaki, K. Matsuoka, T. Minami, S. Morita, N. Noda, N. Ohyabu, S. Okamura, M. Osakabe, H. Suzuki, K. Tanaka, C Takahashi, H. Yamada, I. Yamada and O. Motojima,
Experimental Study of Edge Plasma Structure in Various Discharges on Compact Helical System; Aug. 1996

NIFS-438 A. Komori, N. Ohyabu, S. Masuzaki, T. Morisaki, H. Suzuki, C. Takahashi, S. Sakakibara, K. Watanabe, T. Watanabe, T. Minami, S. Morita, K. Tanaka, S. Ohdachi, S. Kubo, N. Inoue, H. Yamada, K. Nishimura, S. Okamura, K. Matsuoka, O. Motojima, M. Fujiwara, A. Iiyoshi. C. C. Klepper, J.F. Lyon, A.C. England, D.E. Greenwood, D.K. Lee, D.R. Overbey, J.A. Rome, D.E. Schechter and C.T. Wilson,
Edge Plasma Control by a Local Island Divertor in the Compact Helical System; Sep. 1996 (IAEA-CN-64/C1-2)

NIFS-439 K. Ida, K. Kondo, K. Nagaski T. Hamada, H. Zushi, S. Hidekuma, F. Sano, T. Mizuuchi, H. Okada, S. Besshou, H. Funaba, Y. Kurimoto, K. Watanabe and T. Obiki,
Dynamics of Ion Temperature in Heliotron-E; Sep. 1996 (IAEA-CN-64/CP-5)

NIFS-440 S. Morita, H. Idei, H. Iguchi, S. Kubo, K. Matsuoka, T. Minami, S. Okamura, T. Ozaki, K. Tanaka, K. Toi, R. Akiyama, A. Ejiri, A. Fujisawa, M. Fujiwara, M. Goto, K. Ida, N. Inoue, A. Komori, R. Kumazawa, S. Masuzaki, T. Morisaki, S. Muto, K. Narihara, K. Nishimura, I. Nomura, S. Ohdachi, M.. Osakabe, A. Sagara, Y. Shirai, H. Suzuki, C. Takahashi, K. Tsumori, T. Watari, H. Yamada and I. Yamada,
A Study on Density Profile and Density Limit of NBI Plasmas in CHS; Sep. 1996 (IAEA-CN-64/CP-3)

NIFS-441 O. Kaneko, Y. Takeiri, K. Tsumori, Y. Oka, M. Osakabe, R. Akiyama, T. Kawamoto, E. Asano and T. Kuroda,
Development of Negative-Ion-Based Neutral Beam Injector for the Large Helical Device; Sep. 1996 (IAEA-CN-64/GP-9)

NIFS-442 K. Toi, K.N. Sato, Y. Hamada, S. Ohdachi, H. Sakakita, A. Nishizawa, A. Ejiri, K. Narihara, H. Kuramoto, Y. Kawasumi, S. Kubo, T. Seki, K. Kitachi, J. Xu, K. Ida, K. Kawahata, I. Nomura, K. Adachi, R. Akiyama, A. Fujisawa, J. Fujita, N. Hiraki, S. Hidekuma, S. Hirokura, H. Idei, T. Ido, H. Iguchi, K. Iwasaki, M. Isobe, O. Kaneko, Y. Kano, M. Kojima, J. Koog, R. Kumazawa, T. Kuroda, J. Li, R. Liang, T. Minami, S. Morita, K. Ohkubo, Y. Oka, S. Okajima, M. Osakabe, Y. Sakawa, M. Sasao, K. Sato, T. Shimpo, T. Shoji, H. Sugai, T. Watari, I. Yamada and K. Yamauti,
Studies of Perturbative Plasma Transport, Ice Pellet Ablation and Sawtooth Phenomena in the JIPP T-IIU Tokamak; Sep. 1996 (IAEA-CN-64/A6-5)

NIFS-443 Y. Todo, T. Sato and The Complexity Simulation Group,
Vlasov-MHD and Particle-MHD Simulations of the Toroidal Alfvén Eigenmode; Sep. 1996 (IAEA-CN-64/D2-3)

NIFS-444 A. Fujisawa, S. Kubo, H. Iguchi, H. Idei, T. Minami, H. Sanuki, K. Itoh, S. Okamura, K. Matsuoka, K. Tanaka, S. Lee, M. Kojima, T.P. Crowley, Y. Hamada, M. Iwase, H. Nagasaki, H. Suzuki, N. Inoue, R. Akiyama, M. Osakabe, S. Morita, C. Takahashi, S. Muto, A. Ejiri, K. Ida, S. Nishimura, K. Narihara, I. Yamada, K. Toi, S. Ohdachi, T. Ozaki, A. Komori, K. Nishimura, S. Hidekuma, K. Ohkubo, D.A. Rasmussen, J.B. Wilgen, M. Murakami, T. Watari and M. Fujiwara,
An Experimental Study of Plasma Confinement and Heating Efficiency through the Potential Profile Measurements with a Heavy Ion Beam Probe in the Compact Helical System; Sep. 1996 (IAEA-CN-64/C1-5)

NIFS-445 O. Motojima, N. Yanagi, S. Imagawa, K. Takahata, S. Yamada, A. Iwamoto, H. Chikaraishi, S. Kitagawa, R. Maekawa, S. Masuzaki, T. Mito, T. Morisaki, A. Nishimura, S. Sakakibara, S. Satoh, T. Satow, H. Tamura, S. Tanahashi, K. Watanabe, S. Yamaguchi, J. Yamamoto, M.Fujiwara and A. Iiyoshi,
Superconducting Magnet Design and Construction of LHD; Sep. 1996 (IAEA-CN-64/G2-4)

NIFS-446 S. Murakami, N. Nakajima, S. Okamura, M. Okamoto and U. Gasparino,
Orbit Effects of Energetic Particles on the Reachable β–Value and the Radial Electric Field in NBI and ECR Heated Heliotron Plasmas; Sep. 1996 (IAEA-CN-64/CP -6) Sep. 1996

NIFS-447 K. Yamazaki, A. Sagara, O. Motojima, M. Fujiwara, T. Amano, H. Chikaraishi, S. Imagawa, T. Muroga, N. Noda, N. Ohyabu, T. Satow, J.F. Wang, K.Y. Watanabe, J. Yamamoto , H. Yamanishi, A. Kohyama, H. Matsui, O. Mitarai, T. Noda, A.A. Shishkin, S. Tanaka and T. Terai
Design Assessment of Heliotron Reactor; Sep. 1996 (IAEA-CN-64/G1-5)

NIFS-448 M. Ozaki, T. Sato and the Complexity Simulation Group,
Interactions of Convecting Magnetic Loops and Arcades; Sep. 1996

NIFS-449 T. Aoki,
Interpolated Differential Operator (IDO) Scheme for Solving Partial Differential Equations; Sep. 1996

NIFS-450 D. Biskamp and T. Sato,
Partial Reconnection in the Sawtooth Collapse; Sep. 1996

NIFS-451 J. Li, X. Gong, L. Luo, F.X. Yin, N. Noda, B. Wan, W. Xu, X. Gao, F. Yin, J.G. Jiang, Z. Wu., J.Y. Zhao, M. Wu, S. Liu and Y. Han,
Effects of High Z Probe on Plasma Behavior in HT-6M Tokamak; Sep. 1996

NIFS-452 N. Nakajima, K. Ichiguchi, M. Okamoto and R.L. Dewar,
Ballooning Modes in Heliotrons/Torsatrons; Sep. 1996 (IAEA-CN-64/D3-6)

NIFS-453 A. Iiyoshi,
Overview of Helical Systems; Sep. 1996 (IAEA-CN-64/O1-7)